TRPA1 is a major oxidant sensor in murine airway sensory neurons

Bret F. Bessac,[1] Michael Sivula,[1] Christian A. von Hehn,[1] Jasmine Escalera,[1] Lauren Cohn,[2] and Sven-Eric Jordt[1]

[1]Department of Pharmacology and [2]Section of Pulmonary and Critical Care Medicine, Yale University School of Medicine, New Haven, Connecticut, USA.

Sensory neurons in the airways are finely tuned to respond to reactive chemicals threatening airway function and integrity. Nasal trigeminal nerve endings are particularly sensitive to oxidants formed in polluted air and during oxidative stress as well as to chlorine, which is frequently released in industrial and domestic accidents. Oxidant activation of airway neurons induces respiratory depression, nasal obstruction, sneezing, cough, and pain. While normally protective, chemosensory airway reflexes can provoke severe complications in patients affected by inflammatory airway conditions like rhinitis and asthma. Here, we showed that both hypochlorite, the oxidizing mediator of chlorine, and hydrogen peroxide, a reactive oxygen species, activated Ca^{2+} influx and membrane currents in an oxidant-sensitive subpopulation of chemosensory neurons. These responses were absent in neurons from mice lacking TRPA1, an ion channel of the transient receptor potential (TRP) gene family. TRPA1 channels were strongly activated by hypochlorite and hydrogen peroxide in primary sensory neurons and heterologous cells. In tests of respiratory function, *Trpa1*$^{-/-}$ mice displayed profound deficiencies in hypochlorite- and hydrogen peroxide–induced respiratory depression as well as decreased oxidant-induced pain behavior. Our results indicate that TRPA1 is an oxidant sensor in sensory neurons, initiating neuronal excitation and subsequent physiological responses in vitro and in vivo.

Introduction

Chemosensory nerve endings in the airways constantly monitor the chemical composition of the inspired air (1). Airway nerve endings in the nasal passages and bronchi are particularly sensitive to oxidizing chemicals, including peroxides, ozone, oxygen radicals, and chlorine, that pose potential threats to airway function and integrity. Oxidants such as hydrogen peroxide (H_2O_2), ozone, and other reactive oxygen species are among the principal components of photochemical smog, automobile exhaust, tobacco smoke, and smoke from fires (2, 3). They are responsible for many of the acute and chronic respiratory health effects of air pollution. Exposures to the oxidant gas chlorine and reactive chlorine products frequently occur in industrial or domestic accidents and are the most common causes for respiratory irritation and injuries treated in the environmental and occupational health practices (4, 5). Unfortunately, chlorine was also used as a warfare agent and is viewed as a chemical terrorism threat (5, 6). Reactive oxygen species as well as hypochlorite (OCl^-), the oxidizing mediator of chlorine, are also produced endogenously by macrophages and neutrophils during oxidative stress and as a consequence of inhalation of toxic particulates (7–9).

In conscious mice and rats, exposure to very low concentrations of chlorine gas (beginning at <1 part per million [ppm]) or OCl^- aerosols elicits a rapid decline in respiratory rates (10–14). Chlorine also induces nasal obstruction, as shown by invasive measurements in the isolated murine upper respiratory tract (14). Similar nasal responses occur in humans, in which chlorine elicits rapid nasal congestion even at concentrations not consciously perceived as irritating or painful (4, 11, 15–19). In both humans and rodents, nasal responses to chlorine are independent from cholinergic pathways affecting respiratory control and mechanics (14, 17). Injection of capsaicin, which leads to elimination or desensitization of sensory neuronal C-fibers, abolishes these effects, suggesting an important role of sensory neurons in the response to oxidants (14). At low exposure levels, chlorine is cleared with 97.5% efficiency from the air passing through the murine upper respiratory tract (14). Because rodents are obligatory nasal breathers, the chlorine concentration reaching the lower airways is minimal. Thus, respiratory depression is likely caused through interaction with trigeminal chemosensory nerve endings in the nose, and not through bronchoirritation and subsequent changes in lower airway mechanics (14). Similar to murine airways, chlorine is cleared with greater than 95% efficiency in the upper human airways during low-level exposure, with either nasal or oral breathing (20, 21). Other oxidants, including H_2O_2, elicit respiratory responses similar to those of chlorine, including respiratory rate depression (22, 23).

Chemosensory respiratory reflexes triggered in the upper airways are thought to limit exposure of the lower airways to potentially damaging chemicals (15, 24–26). Neuronal activation also triggers airway pain, possibly to induce avoidance behavior, as well as mucus secretion, to buffer or inactivate oxidants. Neurogenic inflammation, mediated by neuropeptides released from airway nerve endings, can further increase airway constriction and sensitize individuals to future oxidant exposures (27–29). When reaching the lower airways in high amounts, oxidants cause bronchoirritation, pain, and oxidative tissue injury, at least in part through activation of bronchial chemosensory nerve endings. While normally fulfilling protective functions, chemosensory airway reflexes and neurogenic inflammatory responses can exacerbate preexisting respiratory conditions. Individuals affected by inflammatory airway conditions such as rhinitis and asthma are frequently sensitized to oxidant exposure (4, 30). In these individuals, even very small

Nonstandard abbreviations used: ANCOVA, analysis of covariance; $[Ca^{2+}]_i$, intracellular Ca^{2+}; DRG, dorsal root ganglia; EEP, end expiratory pause; MV, minute volume; ppm, part(s) per million; TRP, transient receptor potential; TV, tidal volume.

Conflict of interest: The authors have declared that no conflict of interest exists.

Citation for this article: *J. Clin. Invest.* **118**:1899–1910 (2008). doi:10.1172/JCI34192.

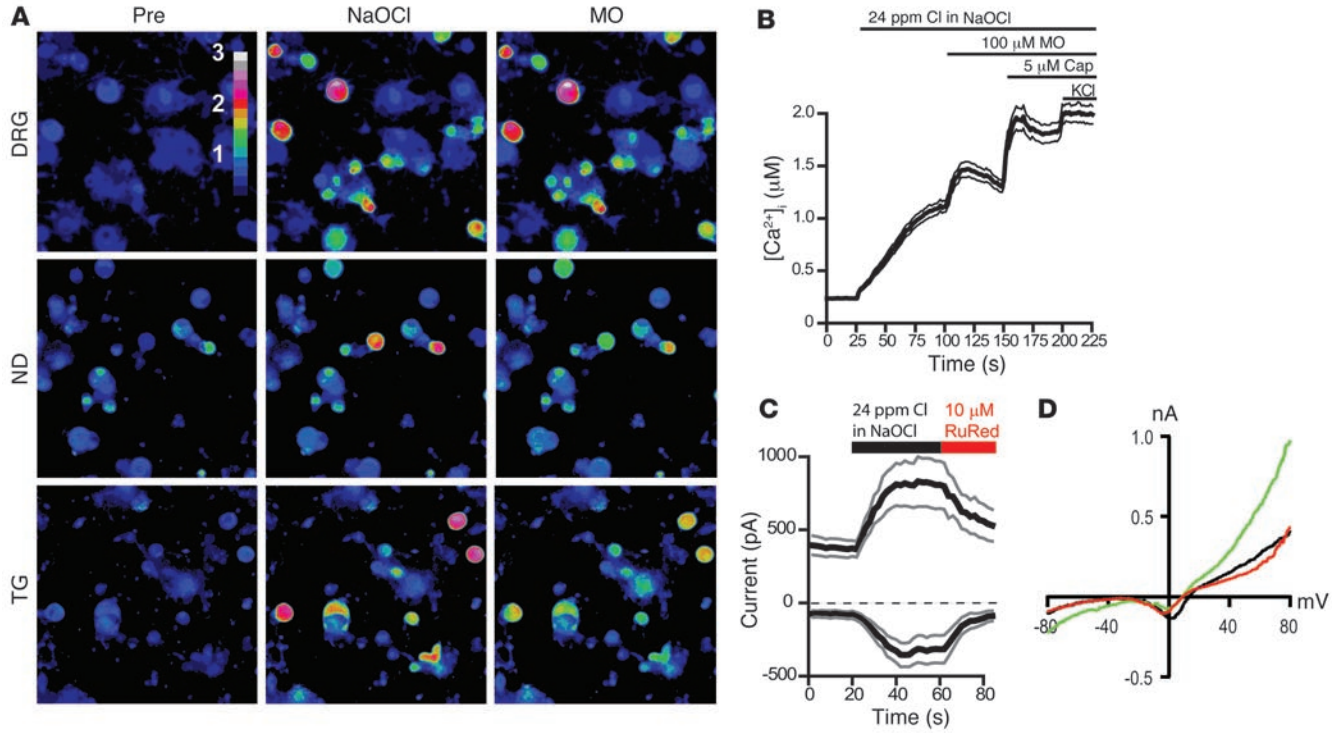

Figure 1

NaOCl induces Ca^{2+} influx and ionic currents in mustard oil–responsive sensory neurons. (**A**) Activation of Ca^{2+} influx into cultured murine DRG, nodose (ND), and trigeminal (TG) neurons by NaOCl, as measured by fluorescent Fura-2 imaging, before and 70 s after challenge with NaOCl (24 ppm), followed by 100 μM mustard oil (MO) after 40 s. Pseudocolors denote 0–3 μM $[Ca^{2+}]_i$. Original magnification, ×10. (**B**) $[Ca^{2+}]_i$ concentration of DRG neurons activated by application of NaOCl followed by mustard oil, capsaicin (Cap), and 65 mM KCl. Thick and thin lines denote mean and ± SEM, respectively. Neurons (n = 300) were analyzed from 4 mice at ×10 magnification. (**C**) Kinetics of OCl^--activated cationic currents and ruthenium red–induced block in cultured murine DRG neurons. NaOCl was superfused after 20 s; after 60 s, ruthenium red (RuRed) was added to the NaOCl. Currents were measured using a ±80 mV voltage ramp protocol over 100 ms at 0.5-Hz intervals (0 mV holding potential throughout). Black and gray lines denote mean and ± SEM, respectively, of currents from 6 neurons at –80 and +80 mV plotted versus time. Intracellular Cs-based solution contained 10 mM EGTA. (**D**) Representative current-voltage relationship of a OCl^--sensitive DRG neuron before application of NaOCl (black), during maximal activation by NaOCl (24 ppm, green), and after application of 10 μM ruthenium red (red). Residual voltage gated currents observed are caused by incomplete inactivation of voltage-gated channels. Currents were measured as in **C**.

amounts of inhaled oxidants can induce strong nasal irritation and obstruction, persistent sneezing, cough, and chest tightness as well as wheezing, dyspnea, and bronchospasm (4, 29–31). Sensitization to oxidants is likely caused by the activation of inflammatory signaling pathways that increase neuronal excitability (26, 29).

In mice, capsaicin-induced ablation or desensitization of sensory C-fibers abolished chlorine- and H_2O_2-induced airway reflexes and nasal constriction (14, 22). These data suggest that nasal trigeminal C-fibers contain specific detection systems for oxidants. C-fibers express a large variety of chemosensory receptors responding to different physical and chemical sensory stimuli, including transient receptor potential (TRP) ion channels, acid-sensitive channels (32, 33), purinergic receptors (34), and potassium and sodium channels (35). While activation of some of these receptors can induce chemosensory airway reflexes, to our knowledge the molecular targets for reactive oxidants have not previously been identified.

In order to gain insight into the mechanism of neuronal oxidant detection, we investigated the effects of oxidants on cultured sensory neurons by ratiometric fluorescent imaging and patch-clamp electrophysiology and in whole animals by studying respiratory responses and pain behavior. We found that OCl^- and the reactive oxygen species H_2O_2 activated Ca^{2+} influx and depolarization in an oxidant-sensitive subpopulation of sensory neurons. These responses were mediated by TRPA1, a chemosensory TRP ion channel involved in inflammatory pain signaling (36–39). Both cloned human and murine TRPA1 channels were strongly activated by chlorine and H_2O_2 in heterologous cells. In *Trpa1*$^{-/-}$ mice, the respiratory effects of OCl^- and H_2O_2 exposure were dramatically diminished. In addition, *Trpa1*$^{-/-}$ mice exhibited greatly diminished pain responses to oxidant stimuli. Thus, we established TRPA1 as a major chemosensory receptor for reactive oxidants in sensory neurons in vitro and in vivo.

Results

OCl^- induces Ca^{2+} influx into mustard oil–sensitive sensory neurons. To study the effects of oxidizing agents on sensory neurons, we first examined the physiological responses of cultured sensory neurons to OCl^-, the oxidizing mediator of chlorine. Chlorine rapidly reacts with water to form hydrochloric acid (HCl) and hypochlorous acid (HOCl). In biological systems, the acidity generated by HCl is readily buffered, which suggests that oxidizing HOCl and its reactive anion, OCl^-, are the main mediators of chlorine's irritancy. Indeed, studies comparing the acute respiratory irritancy of chlorine, HCl fumes, and aerosols containing chlorine bleach (sodium hypochlo-

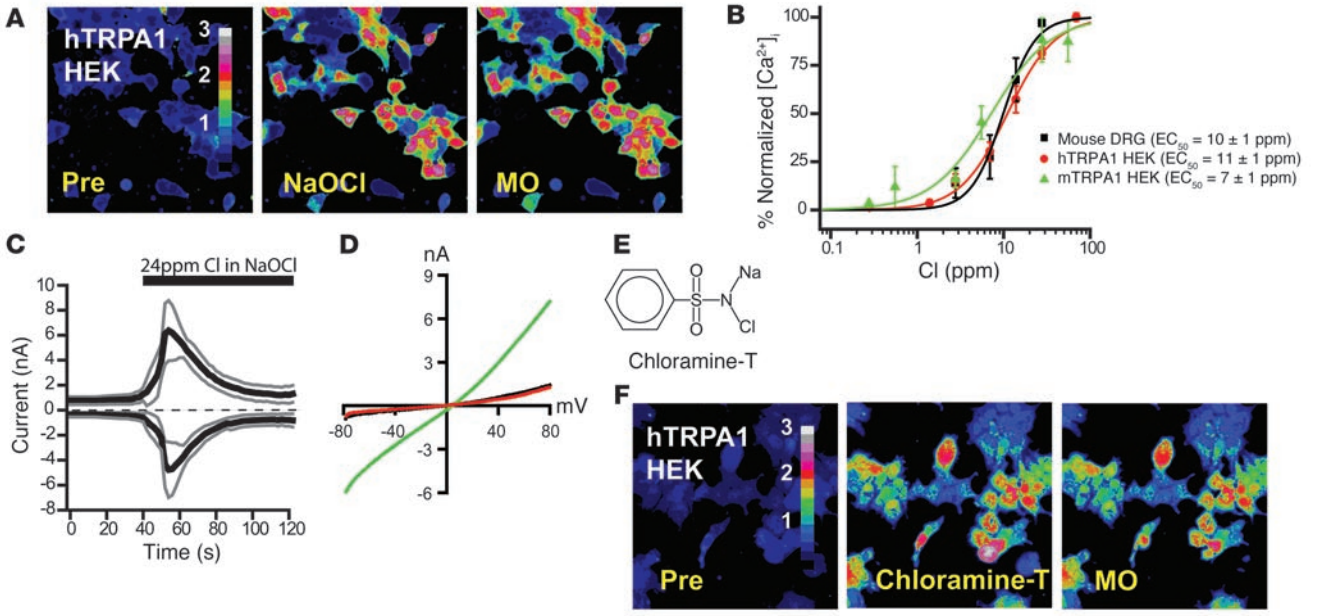

Figure 2

NaOCl activation of cloned TRPA1 channels in HEK293t cells. (**A**) Activation of Ca^{2+} influx into hTRPA1-transfected HEK293t cells by NaOCl (24 ppm) and 100 μM mustard oil. Pre, unstimulated. Pseudocolors denote 0–3 μM $[Ca^{2+}]_i$. (**B**) Dose-response relationship of NaOCl-activated Ca^{2+} influx into cultured DRG neurons (black; $n = 25 \pm 1$ cells/dose), mTRPA1-expressing (green; $n = 23 \pm 5$ cells/dose), and hTRPA1-expressing HEK293t cells (red; $n = 38 \pm 8$ cells/dose). Cells were activated with the indicated concentrations of NaOCl, then with 100 μM mustard oil. Baseline $[Ca^{2+}]_i$ level was subtracted for each cell. Error bars denote SEM. (**C**) Kinetics of NaOCl-induced currents through hTRPA1 channels expressed in HEK293t cells. NaOCl was added to the bath solution after 40 s. Currents were measured using a ±80 mV voltage ramp protocol over 100 ms at 0.5-Hz intervals (0 mV holding potential throughout). Black and gray lines denote mean and ± SEM, respectively, of current amplitudes at –80 and +80 mV plotted versus time ($n = 4$). Intracellular Cs-based solution contained 10 mM EGTA. (**D**) Current-voltage relationship of a representative hTRPA1-transfected HEK293t cell before activation (black), during maximal NaOCl activation (24 ppm; green), and at the end of the inactivation phase (red). (**E**) Chemical structure of chloramine-T. (**F**) Activation of Ca^{2+} influx into hTRPA1-transfected HEK293t cells by 100 μM chloramine-T and 100 μM mustard oil. Pseudocolors denote 0–3 μM $[Ca^{2+}]_i$.

rite, NaOCl) showed that the potency of chlorine is greater than 33-fold that of HCl in causing respiratory depression, whereas NaOCl aerosol is at least as potent as chlorine (10, 14). Both membrane-permeable HOCl and OCl^- are present in biological tissues, because the pK_a of HOCl, at 7.59, is close to physiological pH (40).

We examined the sensory neuronal response to chlorine by intracellular Ca^{2+} ($[Ca^{2+}]_i$) imaging and patch-clamp electrophysiological recordings of cultured murine dorsal root ganglia (DRG) neurons superfused with NaOCl. Cultured neurons were initially exposed to NaOCl-containing physiological buffer. Unless otherwise noted, the NaOCl content was adjusted to a level of 24 ppm total reactive chlorine, as determined photometrically following the standard methodology recommended by the Environmental Protection Agency (EPA) (41). This concentration is considered to make drinking water unpalatable and is about 5-fold the concentration recommended for swimming pool water (41). Strikingly, NaOCl induced a robust increase in $[Ca^{2+}]_i$ in a subpopulation of neurons (Figure 1, A and B). Cultured neurons from trigeminal ganglia, innervating the upper airways, and from nodose ganglia, innervating the bronchi and other parts of the airways, also displayed robust responses to NaOCl (Figure 1A). To further characterize the neuronal samples, we applied 100 μM mustard oil (allyl isothiocyanate) and 5 μM capsaicin, C-fiber–specific sensory irritants activating the Ca^{2+}-permeable ion channels TRPA1 and TRPV1, respectively (Figure 1, A and B) (37, 42, 43). As a final stimulus, 65 mM potassium chloride (KCl) was added to depolarize all neurons, thus activating voltage-gated Ca^{2+} channels. Mustard oil increased Ca^{2+} concentrations in neurons previously challenged with NaOCl. However, mustard oil failed to activate any additional neurons. The OCl^-- and mustard oil–responsive cellular population was 96% ± 4% identical (as tested in 5 fields of DRG neurons, dissociated from 4 different mice). When the sequence of agonists was reversed (100 μM mustard oil followed by NaOCl), NaOCl failed to activate Ca^{2+} influx into additional neurons (95% ± 5% identical; Supplemental Figure 1A; supplemental material available online with this article; doi:10.1172/JCI34192DS1). Neurons initially activated by a nonsaturating dose of mustard oil (33 μM) showed further increases in $[Ca^{2+}]_i$ when superfused with a saturating dose of NaOCl (Supplemental Figure 1B). However, not all C-fiber neurons were sensitive to NaOCl or mustard oil, because capsaicin activated further $[Ca^{2+}]_i$ influx into preactivated cells and activated additional cells that were unresponsive to NaOCl (Figure 1B). The NaOCl-induced rise in $[Ca^{2+}]_i$ was likely caused by influx of extracellular Ca^{2+} into the neuronal cells, because application of NaOCl in Ca^{2+}-free buffer (containing 10 mM EGTA) failed to activate a rise in $[Ca^{2+}]_i$ (Supplemental Figure 1C). To further examine the nature of the neuronal NaOCl-activated Ca^{2+} influx pathway, we measured the effects of NaOCl on neuronal membrane conductance using whole-cell patch-clamp electrophysiology. NaOCl induced a sizable current in 30% (6 of 20) of recorded sensory

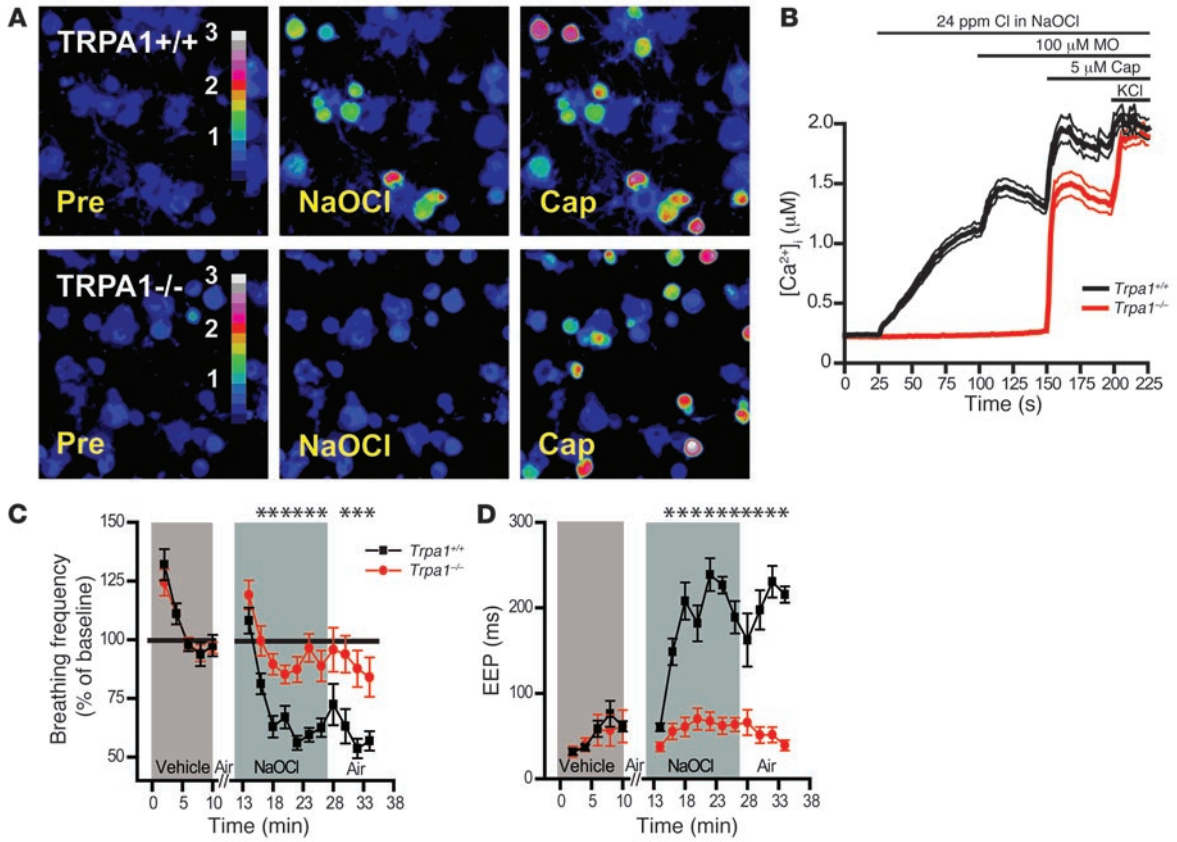

Figure 3

Lack of NaOCl-induced Ca^{2+} influx in sensory neurons and respiratory insensitivity to NaOCl aerosol in *Trpa1*$^{-/-}$ mice. (**A**) Responses of cultured DRG neurons from littermate *Trpa1*$^{+/+}$ and *Trpa1*$^{-/-}$ mice to NaOCl (24 ppm) followed by 5 μM capsaicin, as measured by Fura-2 imaging. *Trpa1*$^{-/-}$ neurons showed no $[Ca^{2+}]_i$ increase after NaOCl exposure, but were activated by capsaicin. Pseudocolors denote 0–3 μM $[Ca^{2+}]_i$. (**B**) Activation of Ca^{2+} influx into DRG neurons plotted against time. Average $[Ca^{2+}]_i$ concentration of neurons activated by application of NaOCl followed by mustard oil, capsaicin, and 65 mM KCl. Thick and thin lines denote mean and ± SEM, respectively. Neurons (n = 300 [*Trpa1*$^{+/+}$]; 263 [*Trpa1*$^{-/-}$]) cultured from 4 mice per group were analyzed at ×10 magnification. (**C**) Effects of exposure to NaOCl aerosol on respiratory frequencies, as measured by unrestrained plethysmography. Mice were exposed to vehicle aerosol (10 min), room air flush (2 min), NaOCl aerosol (15 min), and then air (8 min). Values denote percentage of baseline (initial vehicle exposure). Respiratory frequency was slightly affected in *Trpa1*$^{-/-}$ mice, but dramatically declined in *Trpa1*$^{+/+}$ mice during NaOCl exposure and when NaOCl aerosol was replaced by air. Error bars denote SEM. $P < 0.00005$ between groups; $P < 0.000001$ over time (repeated-measures ANOVA). n = 11 per group. (**D**) EEP duration during exposure to NaOCl aerosol. Data were collected from the experiment described in **C**. Unlike *Trpa1*$^{-/-}$ mice, *Trpa1*$^{+/+}$ mice responded to NaOCl aerosol with an approximately 3-fold increase in EEP duration, which remained elevated 8 min after the end of NaOCl exposure. $P < 0.000001$ between groups, over time, and for the interaction of genotype and time (repeated-measures ANOVA). Single asterisks denote significant differences (Bonferroni post-hoc analysis; $\alpha = 0.05$) for individual time points.

neurons (Figure 1, C and D). We characterized this current further by using pharmacological blockers of known chemosensory receptors. When we tested the effects of 10 μM ruthenium red, a blocker of certain TRP channels including the sensory receptors TRPA1 and TRPV1 (37, 38, 43), we observed robust inhibition of the NaOCl-activated currents (Figure 1, C and D). Ruthenium red also blocked NaOCl-activated Ca^{2+} influx into neurons in imaging experiments (Supplemental Figure 1D). Therefore, we found a significant cellular overlap between mustard oil sensitivity and NaOCl responsiveness in sensory neurons. We concluded that NaOCl-induced neuronal depolarization and Ca^{2+} influx is possibly mediated by a TRP channel–like activity.

The sensory neuronal ion channel TRPA1 is gated by OCl$^-$ *and the chlorine donor chloramine-T.* Mustard oil–sensitive neurons give rise to a subgroup of peripheral chemosensory C-fibers expressing the mustard oil–activated ion channel TRPA1. TRPA1 is expressed in neurons of all major sensory ganglia, including DRG, trigeminal ganglia, and nodose ganglia (38, 44). TRP channels are widely expressed in sensory systems, with a subset of genes expressed specifically in peripheral sensory neurons. In addition to TRPA1, these include the capsaicin receptor, TRPV1, and the cold/menthol receptor TRPM8 (45–47). These ion channels play a crucial role as primary sensors of noxious and innocuous thermal and chemical stimuli. In addition to mustard oil, TRPA1 is activated by other electrophilic chemicals including cinnamic aldehyde, a compound found in cinnamon, allicin, a pungent ingredient in garlic, and acrolein, an environmental toxicant (36, 42, 48, 49). However, it is not known whether oxidants such as chlorine can activate TRPA1 in vitro or in vivo.

The potential role of TRPA1 in the neuronal response to chlorine was therefore examined by testing the effects of NaOCl on

Table 1
Respiratory parameters of *Trpa1*$^{-/-}$ and *Trpa1*$^{+/+}$ mice exposed to NaOCl

Genotype	Exposure	Respiratory frequency (bpm)	TV (ml)	MV (ml/min)	EEP (ms)
Trpa1$^{+/+}$	Vehicle	312 ± 11	0.21 ± 0.01	62 ± 2	59 ± 6
Trpa1$^{+/+}$	NaOCl	205 ± 10^{A}	0.20 ± 0.01	37 ± 2^{A}	194 ± 10^{A}
Trpa1$^{+/+}$	Air	192 ± 11^{A}	0.21 ± 0.01	39 ± 3^{A}	200 ± 14^{A}
Trpa1$^{-/-}$	Vehicle	324 ± 13	0.21 ± 0.01	65 ± 3	57 ± 14
Trpa1$^{-/-}$	NaOCl	291 ± 10	0.19 ± 0.01	57 ± 3	67 ± 10
Trpa1$^{-/-}$	Air	285 ±15	0.20 ± 0.01	59 ± 5	54 ± 8

$^{A}P < 0.05$ vs. *Trpa1*$^{-/-}$, ANCOVA with Bonferroni post-hoc analysis ($\alpha = 0.001$).

cloned human and mouse TRPA1 channels expressed in cultured HEK293t cells by fluorescent Ca^{2+} imaging and patch-clamp electrophysiology. Indeed, NaOCl induced rapid influx of Ca^{2+} into transiently transfected cells expressing human TRPA1 (hTRPA1; Figure 2A). Untransfected cells, as well as cells expressing TRPV1, were unresponsive to NaOCl exposure (data not shown). NaOCl activated Ca^{2+} influx through hTRPA1 into HEK293t cells with an EC_{50} of 11 ± 1 ppm total chlorine (Figure 2B). Murine TRPA1 (mTRPA1) channels were activated at a similar EC_{50} of 7 ± 1 ppm (Figure 2B). NaOCl-activated Ca^{2+} influx into murine sensory neurons within a nearly identical range of concentrations, with an EC_{50} of 10 ± 1 ppm total chlorine (Figure 2B). NaOCl induced sizable currents in hTRPA1-transfected HEK293t cells that desensitized in the continuous presence of the agonist (Figure 2, C and D). Currents and their kinetic properties were very similar to those of previously reported hTRPA1 currents recorded with other agonists in the presence of Ca^{2+} (50, 51). TRPA1-mediated Ca^{2+} influx was also activated by chloramine-T (N-chloro-sodium-p-toluenesulphenamide), a chlorine-releasing chemical widely used as a disinfectant (EC_{50}, 11 ± 1 μM; Figure 2, E and F). Chloramine-T is a strong respiratory irritant and can induce reactive airway conditions (52). Interestingly, the range of chlorine concentrations required for activation of TRPA1 and neurons by chlorine was close to the concentrations required to induce respiratory depression. The measured RD_{50}, the airborne concentration reducing respiratory frequency by 50%, for chlorine in mice varies between 2.3 ppm and 9.3 ppm, depending on strain and other factors (10, 13, 14).

Trpa1$^{-/-}$ *mice lack neuronal responses to* OCl^- *and fail to show* OCl^-*-induced respiratory depression.* By comparing the effects of NaOCl on cultured neurons from *Trpa1*$^{+/+}$ and *Trpa1*$^{-/-}$ mice, we examined whether TRPA1 is essential for the action of chlorine on sensory neurons (Figure 3, A and B). Strikingly, NaOCl-induced Ca^{2+} influx was completely absent in neurons cultured from *Trpa1*$^{-/-}$ mice (Figure 3, A and B). As already described in the present study, neurons dissociated from *Trpa1*$^{+/+}$ mice showed robust responses to NaOCl. *Trpa1*$^{-/-}$ neurons responded well to 5 μM capsaicin, indicating that C-fiber neurons are intact (Figure 3, A and B). These data show that TRPA1 is essential for the cellular response of sensory neurons to NaOCl in vitro.

Next, we sought to determine whether TRPA1 is also essential for sensory neuronal activation by chlorine in vivo. We compared the respiratory responses of *Trpa1*$^{+/+}$ and *Trpa1*$^{-/-}$ mice to NaOCl aerosol exposure by barometric plethysmography, a method used extensively in the study of sensory irritation by chlorine and other irritants (14, 53, 54). Earlier studies using this method showed that mice respond to low-level chlorine or NaOCl aerosol exposure with a rapid decline in respiratory frequency (14). In addition, significant increases in end expiratory pause (EEP; the period of end expiratory flow) were observed (14). Respiratory rate depression and increased EEP are characteristic for nasal irritant responses, as shown by studies examining the effects of chlorine and numerous other sensory irritants (54–59). These changes in respiratory rate and waveform appeared to be induced by upper airway reflexes following activation of nasal trigeminal sensory nerve endings by OCl^- (14).

To closely mimic exposure situations, we exposed conscious mice to NaOCl aerosol in unrestrained plethysmography chambers. As a control, we first exposed the mice to vehicle buffer aerosol (pH 7.3, without NaOCl) to measure aerosol exposure effects and determine baseline values. Both *Trpa1*$^{+/+}$ and *Trpa1*$^{-/-}$ mice responded with a similar decline in respiratory frequency when exposed to the vehicle aerosol after breathing room air (Figure 3C). Similar effects of saline aerosol exposure have been described in previous studies (24). Respiratory frequencies stabilized within 2–3 min and fluctuated minimally until the end of the 10-min control exposure. The exposure system was then flushed with room air for 2 minutes, during which recordings were paused. The intermittent exposure to air restored respiratory frequencies in both *Trpa1*$^{+/+}$ and *Trpa1*$^{-/-}$ mice to the levels observed before vehicle aerosol exposure. Subsequently, the mice were exposed to NaOCl aerosol for 15 min. The airborne reactive chlorine concentration for NaOCl aerosol exposure was adjusted to 6 ppm, a value within the reported range for murine RD_{50} (airborne concentration that reduces respiratory frequency by 50%; ref. 14). Both *Trpa1*$^{+/+}$ and *Trpa1*$^{-/-}$ mice showed an initial decline in respiratory frequencies, as observed with vehicle aerosol (Figure 3C). However, NaOCl exposure caused the respiratory frequencies of *Trpa1*$^{+/+}$ mice to drop to much lower levels than *Trpa1*$^{-/-}$ mice or vehicle buffer aerosol, and the respiratory frequency remained depressed throughout the exposure to NaOCl aerosol (*Trpa1*$^{+/+}$, 66% ± 2% of baseline; *Trpa1*$^{-/-}$, 91% ± 4% of baseline; $P < 0.001$; Table 1). The exposure system was then flushed with room air, but the respiratory frequencies of *Trpa1*$^{+/+}$ mice remained depressed even 8 min after the end of NaOCl exposure (*Trpa1*$^{+/+}$, 63% ± 5% of baseline; *Trpa1*$^{-/-}$, 90% ± 6% of baseline; $P < 0.001$; Figure 3C and Table 1).

During the same experiments, we also recorded other respiratory parameters, including tidal volume (TV), minute volume (MV), and EEP. MV mirrored the dramatic decline in respiratory frequency, while TV remained unchanged throughout the course of the experiment (Table 1). The NaOCl-induced decline in respiratory frequency in *Trpa1*$^{+/+}$ mice was accompanied by a significant increase in the duration of the EEP compared with baseline that remained strongly elevated after removal of NaOCl aerosol. In contrast, *Trpa1*$^{-/-}$ mice showed no significant changes in EEP during or after NaOCl aerosol exposure (Figure 3D and Table 1). Taken together, our plethysmographic measurements accurately reproduced the reported changes in respiratory parameters induced by exposure to NaOCl aerosol in *Trpa1*$^{+/+}$ mice. Moreover, we found that the respiratory responses to NaOCl aerosol were nearly absent in *Trpa1*$^{-/-}$ mice. Apparently, *Trpa1*$^{-/-}$ mice have an impaired ability to sense the irritant NaOCl at a concentration at which *Trpa1*$^{+/+}$ mice show large irritant-induced changes in respiratory frequency and other respiratory parameters.

Trpa1$^{-/-}$ mice were clearly capable of sensing respiratory exposure to other chemical stimuli. We confirmed this by challenging the

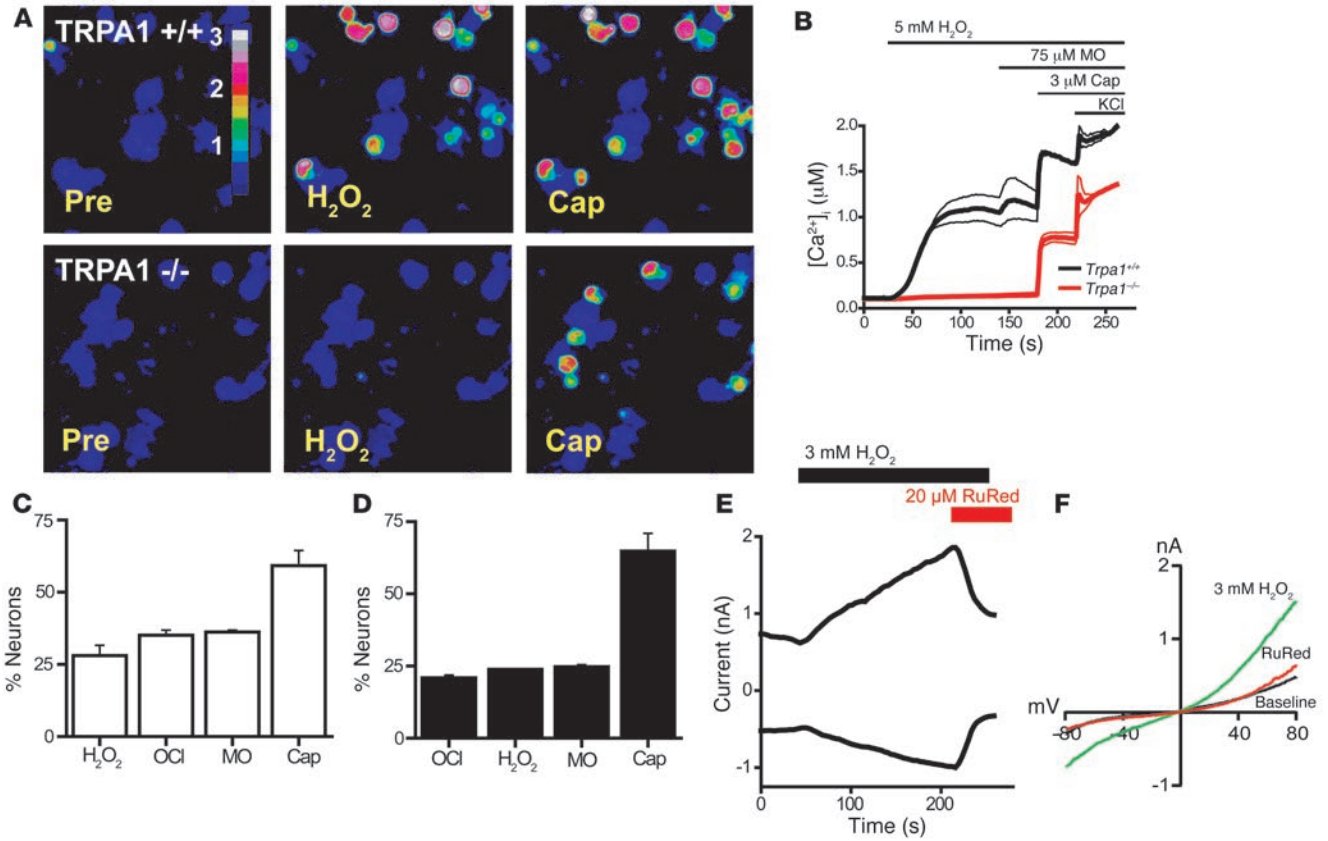

Figure 4

H_2O_2 induces TRPA1-dependent influx of Ca^{2+} and ionic currents in mustard oil–responsive sensory neurons. (**A**) Responses of cultured DRG neurons from littermate *Trpa1*$^{+/+}$ and *Trpa1*$^{-/-}$ mice to 5 mM H_2O_2, followed by 3 μM capsaicin, as measured by Fura-2 imaging. *Trpa1*$^{-/-}$ neurons showed no $[Ca^{2+}]_i$ increase after H_2O_2 exposure, but were activated by capsaicin. Pseudocolors denote 0–3 μM $[Ca^{2+}]_i$. (**B**) Activation of Ca^{2+} influx by H_2O_2 into DRG neurons plotted against time. Average $[Ca^{2+}]_i$ concentration of neurons activated by application of H_2O_2 followed by mustard oil, capsaicin, and 65 mM KCl. Thick and thin lines denote mean and ± SEM, respectively. Neurons (n = 189 [*Trpa1*$^{+/+}$]; 146 [*Trpa1*$^{-/-}$]) were analyzed at ×10 magnification. (**C**) Activation of DRG neurons (n = 161) by 5 mM H_2O_2, NaOCl (24 ppm), 100 μM mustard oil, 5 μM capsaicin, and 65 mM KCl. Neurons were considered activated when $[Ca^{2+}]_i$ exceeded 500 nM. Values denote activated KCl-sensitive cells. (**D**) Activation of DRG neurons (n = 130) by NaOCl (24 ppm), 5 mM H_2O_2, 100 μM mustard oil, 5 μM capsaicin, and 65 mM KCl. (**E**) Kinetics of H_2O_2-activated cationic currents and ruthenium red–induced block in a cultured murine sensory neuron. H_2O_2 was superfused after 50-s initiation of whole-cell configuration, after which ruthenium red was coapplied at 210 s. Currents were measured using a ±80 mV voltage ramp protocol over 100 ms at 0.5-Hz intervals (0 mV holding potential throughout). Intracellular Cs-based solution contained 10 mM EGTA. (**F**) Representative current-voltage relationships of currents recorded from a DRG neuron before application of H_2O_2 (black), during maximal activation by H_2O_2 (green), and after application of 20 μM ruthenium red (red). Currents were measured as in **C**. Error bars represent SEM.

mice with acetic acid aerosol, a known respiratory irritant whose effects are mediated by chemosensory C-fibers (54). When we exposed *Trpa1*$^{-/-}$ mice to acetic acid aerosol, we observed a decline in respiratory frequency and an increase in EEP (Supplemental Figure 2, A and B) similar to data reported in previous studies (54). Thus, absence of TRPA1 does not cause a general defect in sensing of chemical irritants during inhalation.

TRPA1 mediates sensory neuronal responses to H_2O_2. Our initial experiments showed that TRPA1 is the primary target through which the oxidant chlorine excites sensory neurons and activates respiratory depression. In order to determine whether TRPA1 is also a target for other oxidant stimuli, including reactive oxygen species, we examined the effects of H_2O_2 on sensory neuronal activity. Similar to NaOCl, we observed that 5 mM H_2O_2 activated Ca^{2+} influx in a subpopulation of sensory neurons (Figure 4, A and B). Compared with NaOCl, relatively high concentrations of H_2O_2 were required to activate Ca^{2+} influx (>1 mM, or >34 ppm). Subsequent addition of NaOCl or mustard oil failed to activate additional neurons (Figure 4C). Moreover, addition of H_2O_2 to OCl^--exposed neurons also failed to activate additional cells (Figure 4D). H_2O_2-activated Ca^{2+} influx was blocked by ruthenium red (Supplemental Figure 3A). These tests indicated that H_2O_2 activated the OCl^-- and mustard oil–activated subpopulation of sensory neurons that is characterized by expression of TRPA1. Indeed, we found that TRPA1 was crucial for sensory neuronal activation by H_2O_2, because neurons dissociated from *Trpa1*$^{-/-}$ mice showed no observable Ca^{2+} influx in response to H_2O_2 (Figure 4, A and B).

In patch-clamp recordings of sensory neurons, we observed that 3 mM H_2O_2 induced slowly activating ionic currents (Figure 4, E and F). The averaged maximal currents showed slight outward rectification (+80 mV, 0.72 ± 0.12 nA; –80 mV, 0.47 ± 0.04 nA; n = 6

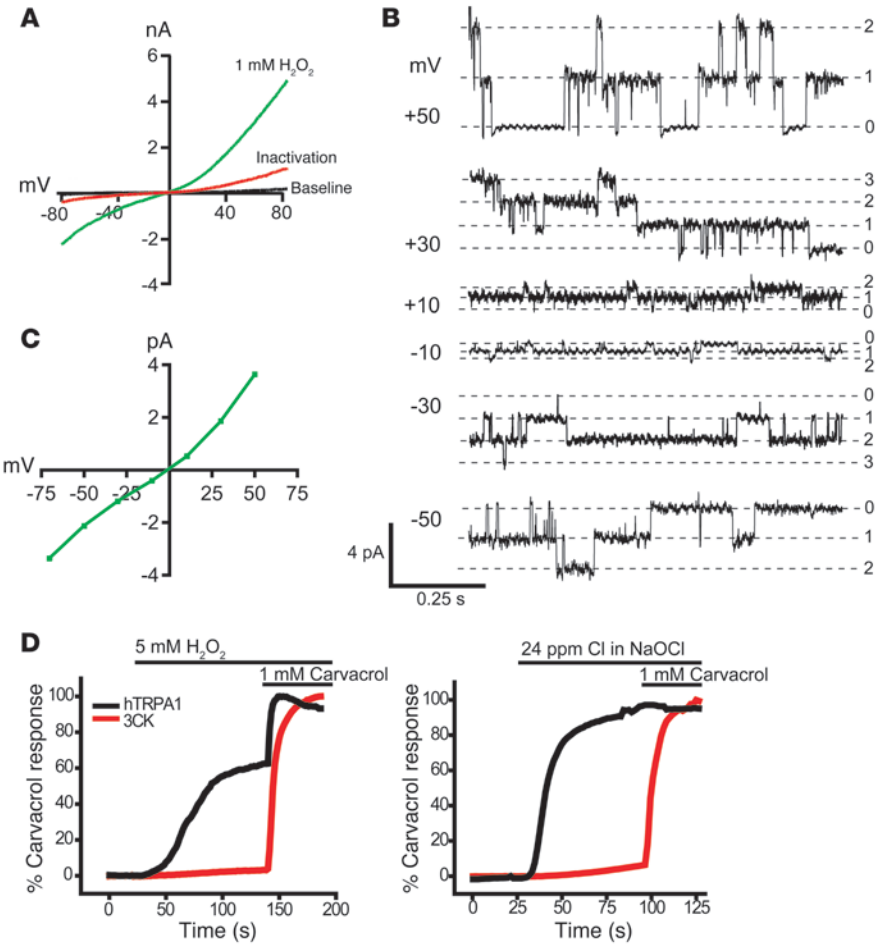

Figure 5

Activation of heterologously expressed TRPA1 channels by H_2O_2. (**A**) Representative whole-cell current-voltage relationship of hTRPA1 currents in CHO cells before activation (black), during maximal activation by H_2O_2 (green), and at the end of the inactivation phase (red). Currents were measured using a ±80 mV voltage ramp protocol over 100 ms at 0.5-Hz intervals (0 mV holding potential throughout). Intracellular Cs-based solution contained 10 mM EGTA. (**B**) Single TRPA1 channel currents induced by H_2O_2 in the cell-attached configuration. Cell-attached patches were formed on CHO cells expressing hTRPA1. The cell was superfused with a bath solution containing 1 mM H_2O_2, and single-channel openings were recorded using a ±60 mV step protocol. Membrane potential was estimated to be –10 mV, where zero currents were observed. Indicated potentials are corrected values. Representative current traces from a patch containing 3 channels are shown. hTRPA1 unitary conductance was 42 ± 0.5 pS (–50 mV) and 73 ± 1.0 pS (+50 mV). Pipette and bath solutions contained 2 mM Ca^{2+}. (**C**) Current-voltage relationship of open channel conductance of single hTRPA1 channels recorded in CHO cells in cell-attached configuration. Values are mean ± SEM of 10 channel openings each. Potentials were corrected as in **B**. (**D**) Requirement of covalent agonist acceptor sites for TRPA1 activation by NaOCl and H_2O_2. $[Ca^{2+}]_i$ changes were compared between HEK293t cells expressing hTRPA1 WT channels and cells expressing TRPA1 channels with mutated interaction sites (C619, C639, C663, and K708; denoted 3CK). A 1-mM dose of nonreactive agonist carvacrol was given after the indicated oxidant stimulus. Values denote percent maximal response to carvacrol (n = 60 cells/trace).

cells). Similar to OCl^--activated currents, these currents were sensitive to block by ruthenium red (Figure 4, E and F).

Subsequent functional tests in heterologous cells confirmed that TRPA1 was indeed activated by H_2O_2 (Figure 5, A–C). In Ca^{2+} imaging experiments, hTRPA1-transfected cells displayed robust Ca^{2+} influx in response to H_2O_2 (EC_{50}, 290 ± 90 μM; data not shown). In patch-clamp experiments, H_2O_2 activated outwardly rectifying currents in hTRPA1-transfected cells (Figure 5A). These currents were absent in mock-transfected cells (data not shown). Maximally activated currents had amplitudes of 3.6 ± 0.6 nA at +80 mV and 1.7 ± 0.3 nA at –80 mV (n = 5 cells). Similar to OCl^--activated currents, H_2O_2-induced currents were inactivated in the presence of agonist and extracellular Ca^{2+} (Figure 5A). Single-channel recordings of TRPA1-transfected cells revealed that H_2O_2 induced channel openings with unitary conductances of 73.0 ± 1.0 pS at +50 mV, and 42 ± 0.5 pS at –50 mV (Figure 5B; see Supplemental Figure 3B for control). The open channels showed outwardly rectifying current-voltage relationships (Figure 5C). Unitary conductances were similar to those of mustard oil–activated TRPA1 channels in the presence of Ca^{2+} (44). Our single-channel recordings were performed in the cell-attached configuration, in which the extracellular face of the membrane patch was occluded from the bath solution by the recording electrode. H_2O_2 was added to the cell through the bath solution. Our observation of robust channel activation in this configuration suggests that the activating stimulus is required to traverse the cell membrane.

Recent studies suggested that electrophilic agonists of TRPA1, including mustard oil and acrolein, activate the channel through covalent modification of cysteine and lysine residues in the cytosolic N terminus of the protein (60, 61). In order to examine the importance of these residues for the activation of TRPA1 by oxidants, we tested the responses of a channel in which reactive cysteine residues and a lysine residue (C619, C639, C663, and K708) were replaced by inert residues (Figure 5D). Carvacrol, a nonreactive agonist of TRPA1, was used as positive control for comparison (62). Intriguingly, the mutant channels failed to respond to both OCl^- and H_2O_2 (Figure 5D). In summary, our data showed that the TRPA1-expressing subpopulation of sensory neurons was excited by both H_2O_2 and OCl^-. Both agonists activated TRPA1 through membrane-traversing pathways dependent on reactive amino acid residues in the channel protein.

$Trpa1^{-/-}$ mice show dramatically reduced respiratory and nocifensive responses to H_2O_2. To examine the role of TRPA1 in the neuronal sensation of airway reactive oxygen species in vivo, we compared the respiratory responses of *$Trpa1^{+/+}$* and *$Trpa1^{-/-}$* mice to H_2O_2 aerosol (Figure 6, A–D). The aerosol was produced from buffered 3% H_2O_2 solution, a concentration widely used for disinfection and bleaching. Similar to earlier reports (22, 23), we observed that exposure to

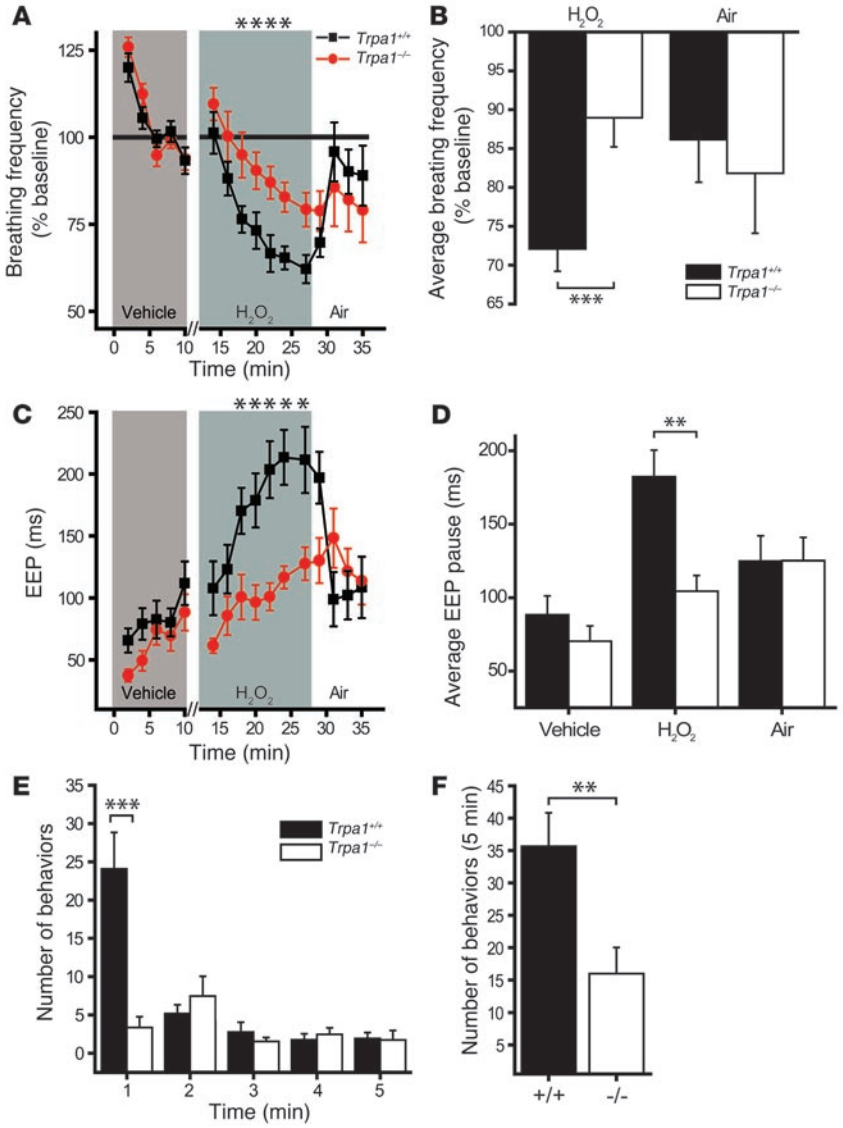

Figure 6
Reduced respiratory and nociceptive sensitivity of *Trpa1*$^{-/-}$ mice to H_2O_2. (**A**) Change in respiratory frequency during aerosol exposure to PBS and 3% H_2O_2, as measured by unrestrained plethysmography. Mice were exposed to vehicle aerosol (10 min), room air flush (2 min), H_2O_2 aerosol (15 min), and then air (8 min). Values denote percent baseline (initial vehicle exposure). Both groups showed a significant decrease in respiratory frequency during H_2O_2 exposure compared with vehicle; however, the reduction in *Trpa1*$^{+/+}$ mice was significantly greater. $P < 0.005$ between groups; $P < 0.000001$ over time (repeated-measures ANOVA). (**B**) Changes in respiratory frequency after exposure to H_2O_2 (2–15 min) and air (8 min) as in **A**. Values denote percent baseline (initial vehicle exposure). (**C**) Changes in EEP duration during exposure to H_2O_2 aerosol as in **A**. $P < 0.001$ between groups; $P < 0.000001$ over time (repeated-measures ANOVA). Single asterisks denote significant differences (Bonferroni post-hoc analysis; $\alpha = 0.05$) for individual time points in **A** and **C**. (**D**) Change in EEP over duration of exposure to vehicle (2–10 min), H_2O_2 (2–15 min), and air (8 min). (**E**) Nocifensive responses following paw injection of 25 μl of 0.1% H_2O_2 solution (32 mM). The number of nocifensive responses (paw flicks, licks, and lifts) was averaged in 1-min intervals. (**F**) Pain responses accumulated over a 5-min period following injection of H_2O_2 as in **E**. (**A**–**D**) $n = 14$ per group. (**E** and **F**) $n = 12$ (*Trpa1*$^{+/+}$), 11 (*Trpa1*$^{-/-}$). Error bars denote SEM. $^{**}P < 0.01$; $^{***}P < 0.001$ (ANOVA).

H_2O_2 aerosol induced depression of respiratory frequencies in wild-type animals (Figure 6, A and B). Respiratory frequencies in *Trpa1*$^{+/+}$ animals were reduced to an average of 72.1% ± 2.9% of baseline during exposure. In contrast, *Trpa1*$^{-/-}$ mice displayed significantly diminished sensitivity to H_2O_2 aerosol (89.0% ± 3.7% of baseline; $P < 0.001$; Figure 6, A and B). H_2O_2-induced respiratory depression occurred at a slower rate than that induced by NaOCl. Similar to NaOCl in *Trpa1*$^{+/+}$ mice, we observed a significant decrease in MV with no significant changes in TV (Table 2). Again, the decrease in respiratory frequency for *Trpa1*$^{+/+}$ mice during H_2O_2 exposure was accompanied by a large increase in EEP (from 88 ± 13 to 182 ± 18 ms; Figure 6, C and D). This parameter was slightly elevated in *Trpa1*$^{-/-}$ mice as well, but significantly lower compared with *Trpa1*$^{+/+}$ mice ($P < 0.001$). In contrast to NaOCl aerosol exposure, respiratory frequency and EEP rapidly recovered following removal of H_2O_2 aerosol (Figure 6, A–D). These data indicate that TRPA1 plays a crucial role for the detection of H_2O_2 in the airways.

In addition to its role as an endogenous reactive oxygen species and environmental toxicant, H_2O_2 is widely used as a topical antiseptic for wound treatment and as a bleaching agent in industrial paper production, detergents, and dental and hair treatments. Painful irritant responses to H_2O_2 have been frequently reported, and application to wounds causes a transient burning sensation. We therefore asked whether TRPA1 would also mediate H_2O_2-induced pain responses. To answer this question, we compared nocifensive responses of *Trpa1*$^{+/+}$ and *Trpa1*$^{-/-}$ mice after injection of 25 μl of 32 mM H_2O_2 solution into the plantar skin of the hind paw (Figure 6, E and F). While *Trpa1*$^{+/+}$ mice displayed paw licking, flicking, and lifting behavior after injection, these behavioral responses were dramatically diminished in *Trpa1*$^{-/-}$ mice (Figure 6, E and F). Differences were especially pronounced immediately after injection, when *Trpa1*$^{+/+}$ mice responded robustly and *Trpa1*$^{-/-}$ mice showed slight responses (Figure 6E). In minutes 2–5 following injection, both *Trpa1*$^{+/+}$ and *Trpa1*$^{-/-}$ mice displayed occasional pain responses, which indicates that H_2O_2 may activate additional delayed pain mechanisms independent of TRPA1 (Figure 6E). These occasional responses were found to be specific to H_2O_2, because PBS-injected mice failed to display any nocifensive responses (data not shown). The difference in nocifensive behavior remained significant over the full 5-minute observation period (Figure 6F). In summary, our

Table 2
Respiratory parameters of *Trpa1*$^{-/-}$ and *Trpa1*$^{+/+}$ mice exposed to H_2O_2

Genotype	Exposure	Respiratory frequency (bpm)	TV (ml)	MV (ml/min)	EEP (ms)
Trpa1$^{+/+}$	Vehicle	309 ± 14	0.20 ± 0.01	59 ± 5	88 ± 13
Trpa1$^{+/+}$	H_2O_2	221 ± 11[A]	0.18 ± 0.01	36 ± 2[A]	182 ± 18[B]
Trpa1$^{+/+}$	Air	260 ± 11	0.18 ± 0.01	46 ± 3	127 ± 18
Trpa1$^{-/-}$	Vehicle	312 ± 11	0.19 ± 0.01	58 ± 3	70 ± 11
Trpa1$^{-/-}$	H_2O_2	274 ± 10	0.20 ± 0.01	51 ± 4	104 ± 11
Trpa1$^{-/-}$	Air	249 ± 19	0.19 ± 0.01	44 ± 3	125 ± 17

[A]$P < 0.05$ vs. *Trpa1*$^{-/-}$ (ANCOVA with Bonferroni post-hoc analysis; $\alpha = 0.001$).
[B]$P < 0.05$ vs. *Trpa1*$^{-/-}$ (ANCOVA with Bonferroni post-hoc analysis; $\alpha = 0.01$).

behavioral analysis showed that TRPA1 is essential for the induction of acute pain responses to H_2O_2.

Discussion

Our data provide what we believe to be the first in vitro and in vivo evidence that TRPA1, an ion channel of the TRP gene family, serves as a major neuronal sensor for oxidants in the airways. We showed that TRPA1 channels in primary sensory neurons and heterologous cells were activated by OCl^- and H_2O_2, a reactive oxygen species. Oxidant activation of TRPA1 occurred within the range of established concentrations for irritancy in humans and rodents. OCl^-- and H_2O_2-induced Ca^{2+} influx was eliminated in cultured neurons from *Trpa1*$^{-/-}$ mice. Cellular insensitivity to oxidants was reflected on the whole-animal level. *Trpa1*$^{-/-}$ mice showed profoundly diminished respiratory responses to low-level chlorine exposure and H_2O_2 exposure. Differences in respiratory sensitivity were specific for oxidants, because responses to a nonoxidizing activator of airway neurons, acetic acid, remained intact in *Trpa1*$^{-/-}$ mice. Diminished oxidant-induced pain behavior in *Trpa1*$^{-/-}$ mice indicated that the role of TRPA1 in oxidant sensing is not restricted to airway neurons, but extends to other peripheral tissues.

TRPA1 was initially identified as a potential sensor for cold temperature and a receptor for plant-derived noxious chemicals including mustard oil, the pungent ingredient in mustard (37, 38, 42). Mustard oil is known as a potent activator of sensory nerve endings in airway mucosa (63). There are several possible mechanisms by which oxidants might activate TRPA1. OCl^- may activate TRPA1 by oxidizing thiols to sulfinate and sulfonate groups or by modifying primary amines (64). Indeed, we found that OCl^- and H_2O_2 failed to activate TRPA1 following mutation of cysteine and lysine residues previously identified as potential acceptor sites for electrophilic agonists (60, 61). Alternatively, oxidants may produce reactive intermediates such as 4-hydroxynonenal, a lipid peroxidation recently found to activate TRPA1 (65). The capabilities of different oxidants to activate TRPA1 may vary widely depending on their reactivity and membrane permeability as well as other factors. This is illustrated by the higher potency and efficacy of OCl^-, a strong oxidant, compared with H_2O_2 for TRPA1 activation and induction of respiratory depression (66). In addition to sensing exogenous oxidants, TRPA1 may also be involved in the detection of endogenous reactive species. Heightened oxidative stress accompanies many inflammatory and painful conditions, including ischemia, neurodegeneration, diabetes, arthritis, and other chronic inflammatory conditions (67–70).

Our results support an essential role for sensory TRPA1 channels in the induction of upper airway irritant responses. Because of the low exposure concentrations used in our study, the observed oxidant-induced respiratory rate depression was likely caused by activation of nasal irritant receptors in trigeminal sensory nerve endings. Our data suggest that oxidants activate TRPA1 channels in nasal trigeminal nerve endings, resulting in neuronal depolarization and activation of neuronal reflexes. In addition, influx of Ca^{2+} through TRPA1 may promote the release of proinflammatory peptides from nasal nerve endings. Sensory neuropeptides such as calcitonin gene–related peptide or substance P are known to induce dilation of blood vessels in the nasal mucosa and promote glandular secretion, contributing to irritant-induced nasal obstruction (71, 72).

In addition to TRPA1, peripheral chemosensory C-fibers express the capsaicin receptor, TRPV1 (37, 38, 44, 73). Similar to oxidants, capsaicin is a potent inducer of respiratory reflex responses and airway obstruction (1). The important role of TRPV1 in the regulation of respiratory reflexes was confirmed by recent pharmacological studies in guinea pigs in which a TRPV1 antagonist displayed antitussive activity (74, 75). TRPA1 is activated by a much broader range of chemical stimuli than TRPV1 and is coexpressed with TRPV1 in chemosensory C-fibers. Recent in vitro studies found that TRPA1 is activated by the α,β-unsaturated aldehyde acrolein, a toxicant in photochemical smog and smoke and a potent activator of respiratory reflexes (49, 76). TRPA1 is also required for the induction of pain responses to formaldehyde and acetaldehyde (77, 78). Our present results support the notion that TRPA1 may mediate respiratory irritant responses to these and many other reactive environmental toxicants in vivo. The existence of a shared neuronal receptor for oxidants and noxious electrophiles, including aldehydes, is also supported by the fact that inhalation of formaldehyde diminishes respiratory irritant responses to subsequent challenges with chlorine and acetaldehyde, and vice versa (12, 79). Cross-tolerance can be explained by the saturation or desensitization of TRPA1 by the different agonists.

Our results showed that sensory neurons derived from the nodose ganglia and DRG, innervating the lower airways, were as sensitive to chlorine as were trigeminal neurons that innervate the nasal passages. These responses were abolished in neurons cultured from *Trpa1*$^{-/-}$ mice. Based on these data, we assume that TRPA1 activation may also contribute to the effects of chlorine and other TRPA1 agonists on chemosensory nerve endings in the lower airways. Because reactive irritants are efficiently cleared in the upper airways, sensory activation in the lower airways requires higher exposure levels. Extended or high-level exposure to oxidants, such as that observed in victims of chlorine gas exposures, induce severe pain, cough, mucus secretion, and bronchospasm (5, 6). At higher exposure levels, oxidants increase TRPA1 activity through direct activation as well as indirectly through phospholipase C–coupled signaling pathways (36). Inhalation of oxidants induces the release of bradykinin, ATP, and lipid products with cognate receptors on airway sensory nerve endings (23, 80). In addition to TRPA1, these mediators may increase the activity of other sensory neuronal detection systems. Indeed, a recent study showed that H_2O_2-induced changes in respiratory frequency can be inhibited, at least in part, by a purinergic receptor antagonist (23). Involvement of additional neuronal pathways may explain why we observed residual respira-

tory depression and pain behavior in *Trpa1*$^{-/-}$ mice in response to the high concentrations of H_2O_2 used in our experiments.

Individuals affected by allergic airway conditions such as rhinitis and asthma often display respiratory hypersensitivity responses to chemical irritants including chlorine, acrolein, and other TRPA1 agonists (4, 54, 81). These exaggerated responses may be the result of sensitization of TRPA1 downstream of neuronal phospholipase C–coupled receptor systems activated during inflammation, including the receptors for bradykinin, histamine, proteases, and other inflammatory stimuli (36, 37, 42, 82, 83). TRPA1 antagonists may be used to suppress sensory neuronal hyperexcitability in airway disease. We conclude that TRPA1 represents a promising new target for the development of drug candidates with potential antitussive, analgesic, and antiinflammatory properties.

Methods

Mice. Mice were housed at an Association for Assessment and Accreditation of Laboratory Animal Care–accredited facility in standard environmental conditions (12-h light/12-h dark cycle; about 23°C). All animal procedures were approved by the Institutional Animal Care and Use Committee of Yale University. Mice were identically matched for age (12–22 weeks) and gender, and the experimenter was blind to the genotype. *Trpa1*$^{-/-}$ mice were a gift from D. Julius (UCSF, San Francisco, California, USA) and were genotyped as previously described (36).

Chemicals and analysis. All irritant chemicals were purchased from Sigma-Aldrich. Total and free chlorine were measured according to the EPA standard 4500-Cl G colorimetric analysis, using N,N-diethy-p-phenylendiamine (PPD-2; HF Scientific Inc.) as a photometric indicator.

Cell culture and transfections. Adult mouse DRG were dissected and dissociated by 1-h incubation in 0.28 WU/ml Liberase Blendzyme 1 (Roche), followed by washes with PBS, trituration, and straining of debris (40-μM Cell Strainer; BD Falcon). Neurons were cultured in neurobasal-A medium (Invitrogen) with B-27 supplement, 0.5 mM glutamine, and 50 ng/ml nerve growth factor (NGF; Calbiochem) on 8-well chambered coverglass or 35-mm cell culture dishes (Nunc) coated with polylysine (Sigma-Aldrich) and laminin (Invitrogen). HEK293t cells for Ca^{2+} imaging and electrophysiology were cultured and transfected as described previously (37).

Ca^{2+} imaging and electrophysiology. Imaging and electrophysiological recordings were performed 16–26 hours after DRG dissection or transfection. Medium was replaced by modified standard Ringer bath solution (140 mM NaCl, 5 mM KCl, 2 mM $CaCl_2$, 2 mM $MgCl_2$, and 10 mM HEPES-NaOH, pH 7.3). Cells were loaded with 10 μM Fura-2/AM (Calbiochem) for 1 h and subsequently washed and imaged in standard bath solution. Ratiometric Ca^{2+} imaging was performed on an Olympus IX51 microscope with a Polychrome V monochromator (Till Photonics) and a PCO Cooke Sensicam QE camera and Imaging Workbench 6 imaging software (Indec). Fura-2 emission images were obtained with exposures of 0.100 ms at 340- and 380-nm excitation wavelengths. $[Ca^{2+}]_i$ concentrations were derived from the F340/F380 ratio adjusted by the K_d of Fura-2 (238 nM) and the F380 and ratiometric data at minimum and maximum $[Ca^{2+}]_i$ (84–86). The latter were determined by incubation of cells in 10 μM ionomycin Ringer solution with no Ca^{2+} and 10 mM EGTA or with 25 mM Ca^{2+} (NaCl 90 mM to compensate for final osmolarity of 350 mOsm). Ratiometric images were generated using ImageJ software (http://rsb.info.nih.gov/ij/). Patch-clamp experiments were performed in the whole-cell or cell-attached configuration with standard Ringer buffer as extracellular solution. Current records were filtered at 2.3 kHz and digitized at 100-μs intervals using an EPC-10 amplifier and PULSEMASTER acquisition software (HEKA). Liquid junction potential was calculated to be 6.7 mV using JPCalc software (Axon Instruments). Both liquid junction potential and capacitance were compensated for using the automatic cancellation features of the EPC-10. Voltage ramps of –80 to +80 mV were applied over 100 ms every other second from a holding potential of 0 mV. Cells were held at 0 mV to inactivate neuronal voltage-gated currents. Current amplitudes were extracted at –80 or +80 mV. Recordings from neurons and CHO cells were performed with Borosilicate glass pipettes (WPI), while a planar patch clamp system was used for recordings from HEK293t cells (NPC-1; Nanion). Both provided an initial series resistance of 3–5 MΩ. Pipette or chip intracellular solution contained 75 mM CsCl, 70 mM CsF, 2 mM $MgCl_2$, 10 mM EGTA, and 10 mM HEPES-CsOH, pH 7.3, 315–320 mOsm. Cell-attached recordings were performed using wax-coated pipettes with an EPC-10 amplifier filtered at 10 kHz with an analog 3-pole Bessel filter and at 2.9 kHz with a 4-pole Bessel filter. Standard Ringer solution was used for bath and pipette solutions in cell-attached recordings. Cell-attached current tracings presented were digitally filtered at 500 Hz. Statistical analysis and graphical display of both electrophysiological and Ca^{2+} imaging data were performed using IGOR PRO (Wavemetrics) or ORIGIN software (OriginLab). Statistical errors are SEM unless indicated otherwise. A freezing point osmometer (Advanced Instruments) was used to measure the osmolality of all solutions.

Respiratory studies. Real-time respiratory responses of mice were measured using unrestrained whole-body plethysmography (Buxco). Respiratory parameters were monitored and analyzed using Buxco Biosystem XA software for noninvasive airway mechanics. For baseline measurements, mice were first exposed to PBS vehicle aerosol for 10 min, followed by NaOCl or 3% H_2O_2 aerosol for 15 min and finally 8 min of room air without aerosol. Solutions for exposure, including vehicle PBS, NaOCl (sodium hypochlorite solution, available chlorine 10%–13%, diluted in PBS; Sigma-Aldrich) and 3% H_2O_2 in PBS, were adjusted to pH 7.3. Solutions were aerosolized with an ultrasonic nebulizer (PulmoSonic), mixed with air in a distribution chamber, and subsequently distributed into 4 parallel unrestrained whole-body plethysmography chambers (Buxco) using the Buxco Aerosol Delivery System (dilution flow, ~3.5 l/min; trickle flow, ~0.3 l/min). For analysis of free reactive chlorine concentration, the NaOCl-air mixture was drawn from the plethysmography chamber through a series of 3 impingers (Kontes-Kimble) containing 40 ml of 1 mM NaOH. After completion of sampling, pH was adjusted to 7.3 with HEPES, and total and free chlorine were measured using EPA standard 4500-Cl G colorimetric analytics (41). The fluid from the last impinger of the series was nearly completely devoid of chlorine, which indicated that all chlorine had been extracted. Respiratory parameters were collected every 10 s for each animal. Four parameters were monitored and averaged: respiratory frequency, TV, MV, and EEP. In accordance with ASTM International protocols, the responses were expressed as follows: TV in ml, MV in ml/min, EEP in absolute values (ms), respiratory frequency as percent of baseline (and as breaths per minute), and Penh normalized to average baseline value and expressed as percent increase over baseline.

Nociceptive behavior. Nocifensive responses (paw flicks, licking, and lifts) were recorded after intraplantar injection of 25 μl H_2O_2 (32 mM in PBS, pH 7.3) into the right hind paw using a 30-gauge needle. Injected mice were immediately placed in a Plexiglas cylinder and videotaped for 5 min. Nocifensive responses were visualized by slowing the video frame speed with Windows Media Player software.

Statistics. For all statistical tests, a P value less than 0.05 was considered significant. Average respiratory frequency (as percent baseline) and average EEP was calculated for each animal in 2-min intervals. Differences between *Trpa1*$^{+/+}$ and *Trpa1*$^{-/-}$ mice during exposure or air were assessed by repeated-measures ANOVA using 2-min respiratory frequency and EEP averages (NCSS software), followed by Bonferroni multiple comparison tests (for 2-factor interactions) to identify specific time points where significant differences between *Trpa1*$^{+/+}$ and *Trpa1*$^{-/-}$ occurred ($\alpha = 0.05$).

For tabular data, individual mouse respiratory frequency, TV, MV, and EEP raw data were averaged for vehicle (2–10 min), exposure (2–15 min), and air flush (8 min) treatments. Average exposure and air data were analyzed by analysis of covariance (ANCOVA), using vehicle averages as the covariate, followed by Bonferroni multiple comparison tests. The degree of significance between *Trpa1*$^{+/+}$ and *Trpa1*$^{-/-}$ mice for exposure or air was examined by varying the α levels of the Bonferroni tests ($\alpha = 0.01$ or 0.001).

Differences in respiratory frequency (percent baseline) and EEP (baseline subtracted) between *Trpa1*$^{-/-}$ and *Trpa1*$^{+/+}$ mice during acetic acid ($n = 4$ per group) and OCl^- ($n = 11$ per group) exposure were examined by 2-way ANOVA followed by Bonferroni multiple comparison tests ($\alpha = 0.05$). The sums of nocifensive paw flick, licking, and lifting responses to H_2O_2 injections were compared between *Trpa1*$^{-/-}$ mice ($n = 11$) and *Trpa1*$^{+/+}$ littermates ($n = 12$) using ANOVA.

Acknowledgments

This work was funded by the NIH Countermeasures Against Chemical Threats (CounterACT) and ONES programs through the National Institute of Environmental Health Sciences (awards U01 ES015674 and R01 ES015056 to S.-E. Jordt and L. Cohn, predoctoral fellowship F31 ES015932 to J. Escalera). Its contents are solely the responsibility of the authors and do not necessarily represent the official views of the federal government. C.A. von Hehn was supported by a Pfizer Patricia Goldman Rakic Award. We are grateful to David Julius for *Trpa1*$^{-/-}$ mice and to Jaime Garcia-Anoveros for mouse TRPA1 cDNA. We thank David Donnelly, James Dziura, James Howe, and Fangyong Li for support.

Received for publication October 10, 2007, and accepted in revised form February 13, 2008.

Address correspondence to: Sven-Eric Jordt, Department of Pharmacology, Yale University School of Medicine, 333 Cedar Street, New Haven, Connecticut 06520, USA. Phone: (203) 785-2159; Fax: (203) 737-2027; E-mail: sven.jordt@yale.edu.

Bret F. Bessac and Michael Sivula contributed equally to this work.

1. Taylor-Clark, T., and Undem, B.J. 2006. Transduction mechanisms in airway sensory nerves. *J. Appl. Physiol.* **101**:950–959.
2. Pryor, W.A., and Stone, K. 1993. Oxidants in cigarette smoke. Radicals, hydrogen peroxide, peroxynitrate, and peroxynitrite. *Ann. N. Y. Acad. Sci.* **686**:12–27; discussion 27–28.
3. Uysal, N., and Schapira, R.M. 2003. Effects of ozone on lung function and lung diseases. *Curr. Opin. Pulm. Med.* **9**:144–150.
4. D'Alessandro, A., Kuschner, W., Wong, H., Boushey, H.A., and Blanc, P.D. 1996. Exaggerated responses to chlorine inhalation among persons with nonspecific airway hyperreactivity. *Chest.* **109**:331–337.
5. Evans, R.B. 2005. Chlorine: state of the art. *Lung.* **183**:151–167.
6. Kilburn, K.H. 2003. Effects of chlorine and its cresylate byproducts on brain and lung performance. *Arch. Environ. Health.* **58**:746–755.
7. Winterbourn, C.C. 2002. Biological reactivity and biomarkers of the neutrophil oxidant, hypochlorous acid. *Toxicology.* **181–182**:223–227.
8. Rhee, S.G. 2006. Cell signaling. H2O2, a necessary evil for cell signaling. *Science.* **312**:1882–1883.
9. Mutlu, G.M., et al. 2006. Airborne particulate matter inhibits alveolar fluid reabsorption in mice via oxidant generation. *Am. J. Respir. Cell Mol. Biol.* **34**:670–676.
10. Barrow, C.S., Alarie, Y., Warrick, J.C., and Stock, M.F. 1977. Comparison of the sensory irritation response in mice to chlorine and hydrogen chloride. *Arch. Environ. Health.* **32**:68–76.
11. Rotman, H.H., et al. 1983. Effects of low concentrations of chlorine on pulmonary function in humans. *J. Appl. Physiol.* **54**:1120–1124.
12. Chang, J.C., and Barrow, C.S. 1984. Sensory irritation tolerance and cross-tolerance in F-344 rats exposed to chlorine or formaldehyde gas. *Toxicol. Appl. Pharmacol.* **76**:319–327.
13. Gagnaire, F., Azim, S., Bonnet, P., Hecht, G., and Hery, M. 1994. Comparison of the sensory irritation response in mice to chlorine and nitrogen trichloride. *J. Appl. Toxicol.* **14**:405–409.
14. Morris, J.B., Wilkie, W.S., and Shusterman, D.J. 2005. Acute respiratory responses of the mouse to chlorine. *Toxicol. Sci.* **83**:380–387.
15. Rupp, H., and Henschler, D. 1967. Wirkungen geringer Chlor- und Bromkonzentrationen auf den Menschen. *Int. Arch. Arbeitsmed.* **23**:79–90.
16. Shusterman, D.J., Murphy, M.A., and Balmes, J.R. 1998. Subjects with seasonal allergic rhinitis and nonrhinitic subjects react differentially to nasal provocation with chlorine gas. *J. Allergy Clin. Immunol.* **101**:732–740.
17. Shusterman, D., Murphy, M.A., Walsh, P., and Balmes, J.R. 2002. Cholinergic blockade does not alter the nasal congestive response to irritant provocation. *Rhinology.* **40**:141–146.
18. Shusterman, D., Murphy, M.A., and Balmes, J. 2003. Influence of age, gender, and allergy status on nasal reactivity to inhaled chlorine. *Inhal. Toxicol.* **15**:1179–1189.
19. Shusterman, D., Balmes, J., Murphy, M.A., Tai, C.F., and Baraniuk, J. 2004. Chlorine inhalation produces nasal airflow limitation in allergic rhinitic subjects without evidence of neuropeptide release. *Neuropeptides.* **38**:351–358.
20. Nodelman, V., and Ultman, J.S. 1999. Longitudinal distribution of chlorine absorption in human airways: a comparison to ozone absorption. *J. Appl. Physiol.* **87**:2073–2080.
21. Nodelman, V., and Ultman, J.S. 1999. Longitudinal distribution of chlorine absorption in human airways: comparison of nasal and oral quiet breathing. *J. Appl. Physiol.* **86**:1984–1993.
22. Ruan, T., Ho, C.Y., and Kou, Y.R. 2003. Afferent vagal pathways mediating respiratory reflexes evoked by ROS in the lungs of anesthetized rats. *J. Appl. Physiol.* **94**:1987–1998.
23. Ruan, T., Lin, Y.S., Lin, K.S., and Kou, Y.R. 2005. Sensory transduction of pulmonary reactive oxygen species by capsaicin-sensitive vagal lung afferent fibres in rats. *J. Physiol.* **565**:563–578.
24. Coleridge, H.M., and Coleridge, J.C. 1994. Pulmonary reflexes: neural mechanisms of pulmonary defense. *Annu. Rev. Physiol.* **56**:69–91.
25. Vesely, K.R., et al. 1999. Capsaicin-sensitive C-fiber-mediated protective responses in ozone inhalation in rats. *J. Appl. Physiol.* **86**:951–962.
26. Lee, L.Y., and Widdicombe, J.G. 2001. Modulation of airway sensitivity to inhaled irritants: role of inflammatory mediators. *Environ. Health Perspect.* **109**(Suppl. 4):585–589.
27. Takebayashi, T., et al. 1998. Role of tachykinins in airway responses to ozone in rats. *J. Appl. Physiol.* **85**:442–450.
28. Wu, Z.X., et al. 2001. Role of intrinsic airway neurons in ozone-induced airway hyperresponsiveness in ferret trachea. *J. Appl. Physiol.* **91**:371–378.
29. Undem, B.J., and Carr, M.J. 2002. The role of nerves in asthma. *Curr. Allergy Asthma Rep.* **2**:159–165.
30. Mapp, C.E., Pozzato, V., Pavoni, V., and Gritti, G. 2000. Severe asthma and ARDS triggered by acute short-term exposure to commonly used cleaning detergents. *Eur. Respir. J.* **16**:570–572.
31. Shusterman, D., Balmes, J., Avila, P.C., Murphy, M.A., and Matovinovic, E. 2003. Chlorine inhalation produces nasal congestion in allergic rhinitics without mast cell degranulation. *Eur. Respir. J.* **21**:652–657.
32. Immke, D.C., and McCleskey, E.W. 2003. Protons open acid-sensing ion channels by catalyzing relief of Ca2+ blockade. *Neuron.* **37**:75–84.
33. Wemmie, J.A., Price, M.P., and Welsh, M.J. 2006. Acid-sensing ion channels: advances, questions and therapeutic opportunities. *Trends Neurosci.* **29**:578–586.
34. Khakh, B.S., and North, R.A. 2006. P2X receptors as cell-surface ATP sensors in health and disease. *Nature.* **442**:527–532.
35. Lai, J., Hunter, J.C., and Porreca, F. 2003. The role of voltage-gated sodium channels in neuropathic pain. *Curr. Opin. Neurobiol.* **13**:291–297.
36. Bautista, D.M., et al. 2006. TRPA1 mediates the inflammatory actions of environmental irritants and proalgesic agents. *Cell.* **124**:1269–1282.
37. Jordt, S.E., et al. 2004. Mustard oils and cannabinoids excite sensory nerve fibres through the TRP channel ANKTM1. *Nature.* **427**:260–265.
38. Story, G.M., et al. 2003. ANKTM1, a TRP-like channel expressed in nociceptive neurons, is activated by cold temperatures. *Cell.* **112**:819–829.
39. Kwan, K.Y., et al. 2006. TRPA1 contributes to cold, mechanical, and chemical nociception but is not essential for hair-cell transduction. *Neuron.* **50**:277–289.
40. Kawai, Y., et al. 2006. Hypochlorous acid-derived modification of phospholipids: characterization of aminophospholipids as regulatory molecules for lipid peroxidation. *Biochemistry.* **45**:14201–14211.
41. Eaton, A.D., Franson, M.A.H., American Public Health Association., American Water Works Association., and Water Environment Federation. 2005. *Standard methods for the examination of water and wastewater*. 21st edition. American Public Health Association. Washington, DC, USA. 1368 pp.
42. Bandell, M., et al. 2004. Noxious cold ion channel TRPA1 is activated by pungent compounds and bradykinin. *Neuron.* **41**:849–857.
43. Caterina, M.J., et al. 1997. The capsaicin receptor: a heat-activated ion channel in the pain pathway. *Nature.* **389**:816–824.
44. Nagata, K., Duggan, A., Kumar, G., and Garcia-Anoveros, J. 2005. Nociceptor and hair cell transducer properties of TRPA1, a channel for pain and hearing. *J. Neurosci.* **25**:4052–4061.
45. Jordt, S.E., McKemy, D.D., and Julius, D. 2003. Les-

sons from peppers and peppermint: the molecular logic of thermosensation. *Curr. Opin. Neurobiol.* **13**:487–492.
46. Clapham, D.E. 2003. TRP channels as cellular sensors. *Nature.* **426**:517–524.
47. Dhaka, A., Viswanath, V., and Patapoutian, A. 2006. Trp ion channels and temperature sensation. *Annu. Rev. Neurosci.* **29**:135–161.
48. Macpherson, L.J., et al. 2005. The pungency of garlic: activation of TRPA1 and TRPV1 in response to allicin. *Curr. Biol.* **15**:929–934.
49. Bautista, D.M., et al. 2005. Pungent products from garlic activate the sensory ion channel TRPA1. *Proc. Natl. Acad. Sci. U. S. A.* **102**:12248–12252.
50. Stokes, A., et al. 2006. TRPA1 is a substrate for deubiquitination by the tumor suppressor CYLD. *Cell Signal.* **18**:1584–1594.
51. Xu, H., Blair, N.T., and Clapham, D.E. 2005. Camphor activates and strongly desensitizes the transient receptor potential vanilloid subtype 1 channel in a vanilloid-independent mechanism. *J. Neurosci.* **25**:8924–8937.
52. Blasco, A., et al. 1992. Bronchial asthma due to sensitization to chloramine T. *J. Investig. Allergol. Clin. Immunol.* **2**:167–170.
53. Vijayaraghavan, R., et al. 1994. Computer assisted recognition and quantitation of the effects of airborne chemicals acting at different areas of the respiratory tract in mice. *Arch. Toxicol.* **68**:490–499.
54. Morris, J.B., et al. 2003. Immediate sensory nerve-mediated respiratory responses to irritants in healthy and allergic airway-diseased mice. *J. Appl. Physiol.* **94**:1563–1571.
55. Alarie, Y. 1973. Sensory irritation of the upper airways by airborne chemicals. *Toxicol. Appl. Pharmacol.* **24**:279–297.
56. Bos, P.M., Zwart, A., Reuzel, P.G., and Bragt, P.C. 1991. Evaluation of the sensory irritation test for the assessment of occupational health risk. *Crit. Rev. Toxicol.* **21**:423–450.
57. Nielsen, G.D. 1991. Mechanisms of activation of the sensory irritant receptor by airborne chemicals. *Crit. Rev. Toxicol.* **21**:183–208.
58. Vijayaraghavan, R., Schaper, M., Thompson, R., Stock, M.F., and Alarie, Y. 1993. Characteristic modifications of the breathing pattern of mice to evaluate the effects of airborne chemicals on the respiratory tract. *Arch. Toxicol.* **67**:478–490.
59. Petak, F., Habre, W., Donati, Y.R., Hantos, Z., and Barazzone-Argiroffo, C. 2001. Hyperoxia-induced changes in mouse lung mechanics: forced oscillations vs. barometric plethysmography. *J Appl Physiol* **90**:2221–2230.
60. Hinman, A., Chuang, H.H., Bautista, D.M., and Julius, D. 2006. TRP channel activation by reversible covalent modification. *Proc. Natl. Acad. Sci. U. S. A.* **103**:19564–19568.
61. Macpherson, L.J., et al. 2007. Noxious compounds activate TRPA1 ion channels through covalent modification of cysteines. *Nature.* **445**:541–545.
62. Xu, H., Delling, M., Jun, J.C., and Clapham, D.E. 2006. Oregano, thyme and clove-derived flavors and skin sensitizers activate specific TRP channels. *Nat. Neurosci.* **9**:628–635.
63. Brand, G., and Jacquot, L. 2002. Sensitization and desensitization to allyl isothiocyanate (mustard oil) in the nasal cavity. *Chem. Senses.* **27**:593–598.
64. Pereira, W.E., Hoyano, Y., Summons, R.E., Bacon, V.A., and Duffield, A.M. 1973. Chlorination studies. II. The reaction of aqueous hypochlorous acid with alpha-amino acids and dipeptides. *Biochim. Biophys. Acta.* **313**:170–180.
65. Trevisani, M., et al. 2007. 4-Hydroxynonenal, an endogenous aldehyde, causes pain and neurogenic inflammation through activation of the irritant receptor TRPA1. *Proc. Natl. Acad. Sci. U. S. A.* **104**:13519–13524.
66. Hammerschmidt, S., and Wahn, H. 2004. The oxidants hypochlorite and hydrogen peroxide induce distinct patterns of acute lung injury. *Biochim. Biophys. Acta.* **1690**:258–264.
67. Andersen, J.K. 2004. Oxidative stress in neurodegeneration: cause or consequence? *Nat. Med.* **10**(Suppl.):S18–S25.
68. Feldman, E.L. 2003. Oxidative stress and diabetic neuropathy: a new understanding of an old problem. *J. Clin. Invest.* **111**:431–433.
69. Mapp, P.I., Grootveld, M.C., and Blake, D.R. 1995. Hypoxia, oxidative stress and rheumatoid arthritis. *Br. Med. Bull.* **51**:419–436.
70. Michel, P.P., Ruberg, M., and Hirsch, E. 2006. Dopaminergic neurons reduced to silence by oxidative stress: an early step in the death cascade in Parkinson's disease? *Sci. STKE.* **2006**:pe19.
71. Petersson, G., Malm, L., Ekman, R., and Hakanson, R. 1989. Capsaicin evokes secretion of nasal fluid and depletes substance P and calcitonin gene-related peptide from the nasal mucosa in the rat. *Br. J. Pharmacol.* **98**:930–936.
72. Baraniuk, J.N., et al. 1990. Calcitonin gene-related peptide in human nasal mucosa. *Am. J. Physiol.* **258**:L81–L88.
73. Watanabe, N., et al. 2005. Immunohistochemical localization of vanilloid receptor subtype 1 (TRPV1) in the guinea pig respiratory system. *Pulm. Pharmacol. Ther.* **18**:187–197.
74. McLeod, R.L., et al. 2006. TRPV1 antagonists attenuate antigen-provoked cough in ovalbumin sensitized guinea pigs. *Cough.* **2**:10.
75. McLeod, R.L. Correll, C.C. Jia, Y. and Anthes, J.C. 2007. TRPV1 antagonists as potential antitussive agents. *Lung*. In press.
76. Morris, J.B., Stanek, J., and Gianutsos, G. 1999. Sensory nerve-mediated immediate nasal responses to inspired acrolein. *J. Appl. Physiol.* **87**:1877–1886.
77. McNamara, C.R., et al. 2007. TRPA1 mediates formalin-induced pain. *Proc. Natl. Acad. Sci. U. S. A.* **104**:13525–13530.
78. Bang, S., Kim, K.Y., Yoo, S., Kim, Y.G., and Hwang, S.W. 2007. Transient receptor potential A1 mediates acetaldehyde-evoked pain sensation. *Eur. J. Neurosci.* **26**:2516–2523.
79. Babiuk, C., Steinhagen, W.H., and Barrow, C.S. 1985. Sensory irritation response to inhaled aldehydes after formaldehyde pretreatment. *Toxicol. Appl. Pharmacol.* **79**:143–149.
80. Shin, J., et al. 2002. Bradykinin-12-lipoxygenase-VR1 signaling pathway for inflammatory hyperalgesia. *Proc. Natl. Acad. Sci. U. S. A.* **99**:10150–10155.
81. Leikauf, G.D., Leming, L.M., O'Donnell, J.R., and Doupnik, C.A. 1989. Bronchial responsiveness and inflammation in guinea pigs exposed to acrolein. *J. Appl. Physiol.* **66**:171–178.
82. Kim, B.M., Lee, S.H., Shim, W.S., and Oh, U. 2004. Histamine-induced Ca(2+) influx via the PLA(2)/lipoxygenase/TRPV1 pathway in rat sensory neurons. *Neurosci. Lett.* **361**:159–162.
83. Dai, Y., et al. 2007. Sensitization of TRPA1 by PAR2 contributes to the sensation of inflammatory pain. *J. Clin. Invest.* **117**:1979–1987.
84. Grynkiewicz, G., Poenie, M., and Tsien, R.Y. 1985. A new generation of Ca2+ indicators with greatly improved fluorescence properties. *J. Biol. Chem.* **260**:3440–3450.
85. Zhou, Z., and Neher, E. 1993. Mobile and immobile calcium buffers in bovine adrenal chromaffin cells. *J. Physiol.* **469**:245–273.
86. Kao, J.P. 1994. Practical aspects of measuring [Ca2+] with fluorescent indicators. *Methods Cell Biol.* **40**:155–181.